ELSEVIER

Journal of Alloys and Compounds 239 (1996) 55–62

Journal of ALLOYS AND COMPOUNDS

YBCO thick films on alumina substrates with sprayed YSZ buffer layers

Yoshiharu Matsuoka[a], Eriko Ban[a], Hirotaka Ogawa[b], Kazuyoshi Kurosawa[c]

[a]*Department of Physics, Meijo University, Tenpaku-ku, Nagoya 468, Japan*
[b]*Department of Transport Machine Engineering, Meijo University, Tenpaku-ku, Nagoya 468, Japan*
[c]*Industrial Research Institute, Aichi Prefectural Government, Nishishinwari, Hitotsugi-cho, Kariya 448, Japan*

Received 24 November 1995; in final form 3 January 1996

Abstract

YBCO thick films of 10–30 μm thickness were fabricated on polycrystalline alumina substrates using a simple screen-printing method. All films on bare alumina substrate showed very poor or non-superconducting properties above 77 K due to aluminium diffusion from the substrate into the film. We have therefore fabricated yttria-stabilized-zirconia (YSZ) buffer layers on alumina substrates by the screen-printing method or by spraying a suspension consisting of ultrafine YSZ powders. The sprayed buffer layers showed a dense and less cracked structure compared with the screen-printed layers, and were found to act as a successful buffer to aluminium diffusion. The J_c values of YBCO films on sprayed layers, fired by the solid-phase sintering method and the liquid-phase processing method, were about 400 and 1300 A cm^{-2} respectively at 77 K, 0 T. These values are about two-thirds of those for films on single-crystal YSZ substrates.

Keywords: High-T_c superconductors; Y–Ba–Cu–O; Thick films; Sprayed buffer layers

1. Introduction

The recent discovery of high-T_c superconductivity in metallic oxides has generated unprecedented research interest. For many applications, such as magnetic shielding, microwave technology and microelectronics, it is important to establish the fabrication technique for high quality thick films of superconducting materials. Various techniques have been used to achieve this [1–6], of which screen-printing is a low-cost and non-vacuum technique, permitting easy patterning on a substrate regardless of its area. $Y_1Ba_2Cu_3O_{7-x}$ (YBCO) thick films have been fabricated on a number of different substrates, including alumina, MgO, $SrTiO_3$, yttria-stabilized-zirconia (YSZ), silicon and various kinds of metal [7–14]. The most successful results so far have been obtained with YBCO thick films processed on YSZ substrates. Unfortunately, YSZ substrates are very expensive and the dielectric losses are high, which makes them generally unsuitable for use as microwave applications.

Alumina substrates are used extensively in electronic devices because of their low cost, required strength, high thermal conductivity and low dielectric losses. There have therefore been a number of attempts to produce high-T_c superconductor thick films on these substrates. YBCO thick films on alumina substrates have, however, very poor superconducting properties due to interdiffusion, chemical reactions and the misfit in expansion coefficients between film and substrate [15–17]. To overcome this difficulty, the following routes have been taken: (i) use of a buffer between YBCO films and the substrate [18], and (ii) making the film thicker (100–200 μm) by painting YBCO paste repeatedly on the substrate [19,20]. Owing to these achievements, the superconducting properties of thick films on alumina have been considerably improved. The best J_c value obtained so far is about 100–200 A cm^{-2} at 77 K, 0 T [18,19]. This value is, however, significantly lower than those measured on YSZ substrates.

In previous papers [21,22], we reported that firing under a flowing rare gas is very useful for the enhancement of the critical current density of films. Here we intend to report the successful preparation of YBCO films of 10–30 μm thickness on YSZ-buffered alumina

Elsevier Science S.A.
PII S0925-8388(96)02240-2

substrates through heat-treatment under flowing argon.

2. Experimental procedure

Two different grades of polycrystalline alumina (Nippon Kagaku Togyo), 93% and 99.5%, and alumina green tape of 99.5% purity (Sumitomo Metal Ceramics, AT-3995-1) have been used as substrates. The main impurity contained in 93% alumina is SiO_2. The ultrafine zirconia powders used in this study (Osaka Cement, OZC-8YA and OZC-8YC) were stabilized with 8 mol.% yttria.

The YSZ buffer layers were processed by the following two methods before printing of YBCO thick films.

(i) The ultrafine YSZ powder (OZC-8YC, mean diameter of crystallite $d = 370$ Å, specific surface $S = 10\,m^2\,g^{-1}$) was mixed with an organic vehicle (Tanaka-Matthey K.K., TMC-10TA) in the weight ratio YSZ:vehicle = 1:1 (1:6 volume ratio) to form a paste. This was printed through a 150 mesh stainless screen onto the 99.5% alumina and alumina green tapes. The YSZ layers formed on the green tapes, which enabled a weak pressure to be applied without any damage because of their elasticity, were then cold pressed at 50 kg cm^{-2} to make the surface smooth and dense. After drying in an oven at 140 °C for 45 min, the buffer layers were fired at 1450 °C for 10 min with heating and cooling rates of 5 °C min^{-1}. The fired layer thickness was found, from SEM observation and/or a surface profile meter, to be about 15 μm.

(ii) The ultrafine YSZ powders (OZC-8YA, $d = 190$ Å, $S = 30\,m^2\,g^{-1}$) were mixed with ethanol in the weight ratio 1:10 for 30 min in an ultrasonic cleaner. The suspension thus prepared was finely sprayed onto 93% and 99.5% alumina substrates through a commercially available nozzle using air as the carrier gas. The spray rate was 0.8 ml min^{-1} and the deposition rate, calculated by dividing the fired YSZ layer thickness by the spraying time, was typically 5×10^3 Å min^{-1}. After that, the YSZ layer was fired at 1400 °C for 10 min with heating and cooling rates of 5 °C min^{-1}. The layer thickness was controlled by changing the amount of spraying suspension.

The preparation methods of YBCO thick films are similar to those described in our other articles [21,22]. A brief description is given here. The paste, prepared by mixing the YBCO powder and an organic vehicle in an agate mortar, was printed through 150 or 300 mesh stainless screen onto the substrates. The YBCO films thus prepared were then fired by the following methods.

(i) *Solid-phase sintering method.* A schematic diagram of the firing schedule is shown in Fig. 1. The

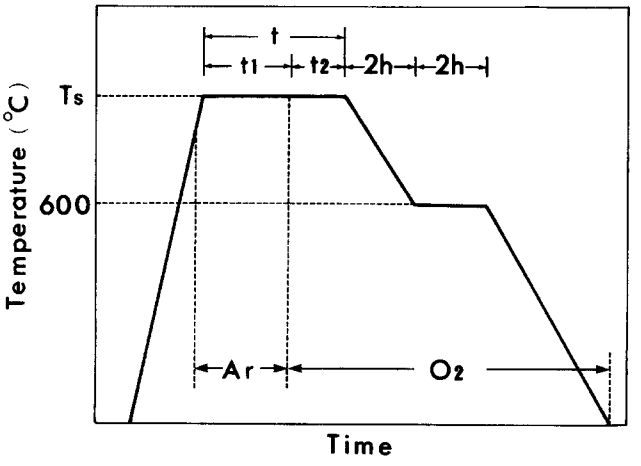

Fig. 1. Schematic diagram of the firing schedule for the preparation of YBCO thick films.

films were fired at the desired firing temperature T_s, 920–980 °C in steps of 10 °C, for a period of time t ($t = t_1 + t_2$). The film was exposed to argon flow (1 l min^{-1}), which was prepassed 20 min before the furnace temperature reached T_s, for a time t_1 and then exposed to oxygen flow (0.5 l min^{-1}) for a time t_2. The furnace was then cooled, with post-annealing at 600 °C for 2 h, to room temperature in flowing oxygen. The fired film thicknesses prepared through 300 and 150 mesh screen were found, using a surface profile meter, to be about 10–15 μm and 25–30 μm respectively.

(ii) *Liquid-phase processing method.* The firing method is almost the same as that used in the previous study [22]: the YBCO film was introduced over a period of 1 min into the center of the tube furnace under flowing argon, which was preheated to the desired firing temperature T_s (1010–1060 °C). After the films had been fired at T_s for 2 min, the furnace was cooled gradually. When the furnace temperature fell to 1010 °C, the flowing gas was changed from argon to oxygen. After this, the films were gradually cooled in the same manner as for the solid-phase sintering method. The fired film thickness prepared through 300 mesh screen was about 10 μm.

The resistivity and critical current density J_c at 77 K, 0 T were measured by a standard d.c. four-probe method. The microstructure of the films was studied using SEM, X-ray diffraction (XRD), energy-dispersive X-ray analysis (EDXA) and electron probe microanalysis (EPMA).

3. Experimental results and discussion

3.1. Solid-phase sintering method

3.1.1. YBCO films on bare alumina substrates

The YBCO films on bare 99.5% alumina substrates were fired at T_s = 920–980 °C in steps of 10 °C for the

firing time $t = 2$ min ($t_2 = 0$). For the films with 10–15 μm thickness, no film gave zero resistivity above 77 K. When the thickness of the film increased to 25–30 μm, either by using 150 mesh screen or painting the YBCO paste twice through 300 mesh, five kinds of sample fired at $T_s = 920$–960 °C attained zero resistivity at T_c (end point) = 80–88 K. The room-temperature resistivity ρ and the J_c values of these samples were, respectively, 7.5–12.5 mΩ cm and less than 4 A cm^{-2}. For the $T_s = 970$ and 980 °C films, in contrast, the ρ values were larger than 25 mΩ cm due to the film poisoning which will be mentioned later, and a critical temperature above 77 K could not be observed.

Fig. 2(a) presents a surface SEM image of the 20–25 μm YBCO film fired at $T_s = 950$ °C. The inset to Fig. 2(a) gives the EDXA over the whole region of the SEM image. Fig. 2(b) shows the XRD pattern (2θ = 31°–34°) of the same sample as in Fig. 2(a). The following features can be seen in these figures. (i) Considering the fact that the Al element of about 8 at.% was detected by EDXA, Al exists near the surface of the film. (ii) The molar Y:Ba:Cu ratio of this region is about 1:1:2, i.e. stoichiometric deviation from the (123) phase occurs. (iii) The distinct doublets owing to the orthorhombic structure around $2\theta = 32°$–33°, i.e. (013), (110) and (103), cannot be observed in the XRD patterns. (iv) The impurity peaks corresponding to Y_2BaCuO_5 (211) are observed, although this is not shown in the figure.

Fig. 3 shows a cross-sectional SEM view and EPMA mapping of Al, Y, Ba, Cu and O of the film fired under the same conditions as in Fig. 2. Element profiles were also analyzed on-line. Several features are noticeable in this figure: (i) though only slightly, the concentration of Al inside the YBCO film decreases gradually on approaching the surface of the film, as also confirmed by EDXA. This implies that Al ions diffuse from the substrate up to the near-surface region of the film. (ii) The Cu-rich regions where both Y and Ba are poor, therefore inferred to be CuO [22], are present over a fairly large region. (iii) The Ba-rich thin layer is seen in the substrate-film interface region. This layer would be $BaAl_2O_4$ produced by the diffusion of Al, Ba and probably O into the interface. In fact, distinct peaks corresponding to $BaAl_2O_4$ ($2\theta = 28.1°$, 34.2°) were observed in the samples polished mechanically up to near the interface. Features similar to (i)–(iii) are also observed in the film fired at the lower temperature of $T_s = 920$ °C. These results are considered to be due to the following reaction [23]:

$$Y_1Ba_2Cu_3O_7 + Al_2O_3 \rightarrow Y_2BaCuO_5 + CuO + BaAl_2O_4 + O_2 \quad (1)$$

The very poor or non-superconducting properties of the film on bare alumina substrates, therefore, may be mainly due to the diffusion of aluminium into the YBCO film, which leads to the stoichometric deviation from the (123) phase and also leads to oxygen depletion from the superconducting YBCO regions [24].

3.1.2. YBCO films on YSZ buffer layers

Figs. 4(a) and 4(b) show XRD patterns and surface SEM images of the YSZ buffer layers formed on 99.5% alumina substrates by the screen-printing and spraying methods respectively. The fired buffer layer thickness of these samples was about 15 μm.

For the screen-printed buffer layer: (i) a number of large cracks remain over the whole surface region. Some of these cracks were produced at the initial drying process of 140 °C due to burn-out of the organic vehicle. The number and size of the cracks increased

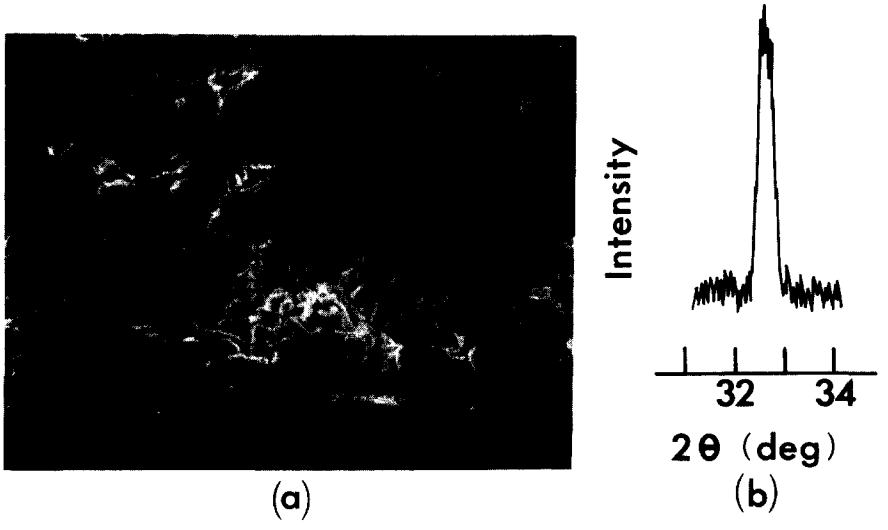

Fig. 2. Surface SEM image and X-ray diffraction profile around 32° to 33° of YBCO thick film on bare alumina substrate fired at $T_s = 950$ °C for $t = 2$ min ($t_2 = 0$). The inset shows the EDXA for the whole region of the SEM image.

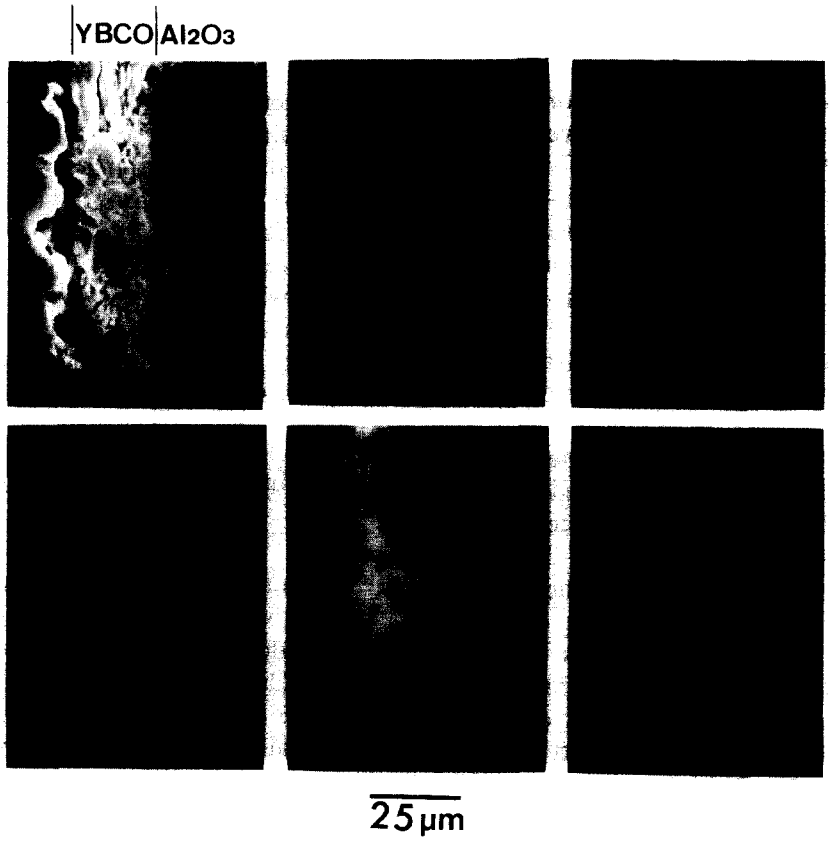

Fig. 3. Cross-sectional SEM view and EPMA mapping of Al, Y, Ba, Cu and O for the YBCO thick film on bare alumina substrate fired at $T_s = 950\,°C$ for $t = 2$ min ($t_2 = 0$). Element profiles are analyzed on-line.

after firing at 1450 °C. From the high magnification SEM photograph, it was found that the central region of some of the large cracks, for example the region marked A in Fig. 4(a), is the surface of the alumina substrate itself. (ii) The distinct peaks of yttrium zirconium oxide and alumina are observed in the XRD patterns. Since the buffer layer fabricated by this method is porous, the diffusion of Al along the grain boundary would be enhanced. The peaks of Al_2O_3 in Fig. 4(a) are therefore inferred to be reflections from the alumina produced by diffusion of some of the Al into the near-surface region and/or from a region such as that marked A. (iii) The average Vickers hardness value measured on 10 points of the surface was 3.6×10^2 HV 0.05.

For the sprayed buffer layer: (i) the buffer layer is highly dense and almost free from large cracks, although some small cracks and a circular pattern (B) formed by spraying the small droplets onto the substrate are present. (ii) The reflections corresponding to the Al_2O_3 phase are significantly less. This suggests that the diffusion of aluminium is suppressed due to the dense structure of the buffer layer. (iii) The average Vickers hardness value on 10 points was 1.2×10^3 HV 0.05. This value is about three times as large as that of the screen-printed layer.

For the screen-printed buffer layers on alumina green tape, the XRD patterns and surface SEM image were similar to those of the screen-printed layers on 99.5% alumina, except for the following two points: first, the length for cracks was slightly greater; second, the average Vickers hardness value was 1.0×10^3 HV 0.05, becoming almost the same as that of the sprayed layer due to the cold pressing.

We next studied the effects of the thickness of the sprayed buffer layer on the superconducting properties. Fig. 5 shows the critical current density J_c of 20–25 μm YBCO films as a function of thickness of buffer layer on two kinds of substrate, 93% and 99.5% alumina. Here the YBCO films on these buffered substrates were fired at $T_s = 950\,°C$ for $t = 2$ min ($t_2 = 0$). It is found from this figure that (i) no significant difference in J_c value between 93% and 99.5% alumina substrates can be seen; (ii) the J_c values increase abruptly to 150 A cm^{-2} or larger when the layer thickness increases up to 8 μm and become almost constant at about 300 A cm^{-2} for layers more than 30 μm thick. These results imply that buffer layers more than 30 μm thick act as a successful barrier to aluminium diffusion. We therefore kept the thickness of sprayed buffer layer constant at 30 μm hereafter.

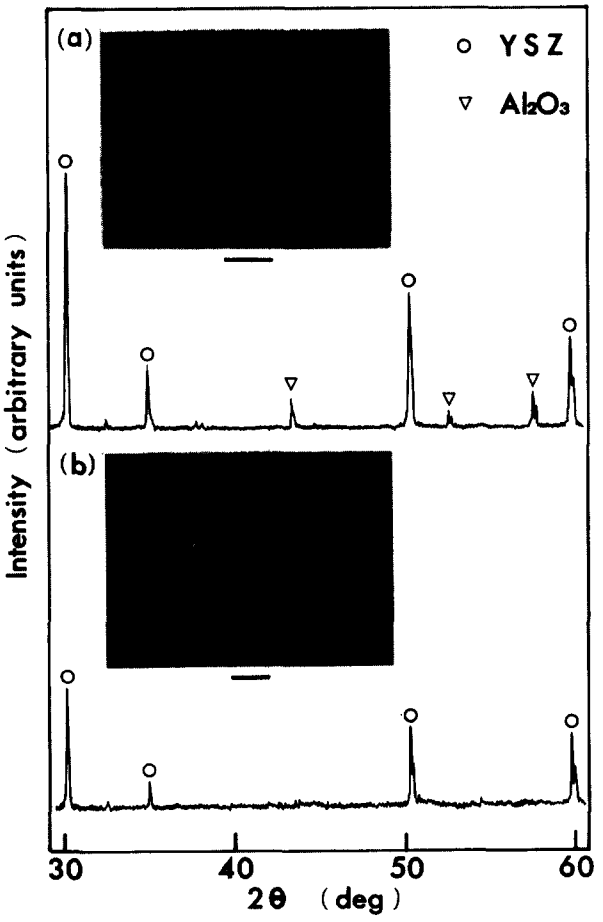

Fig. 4. X-diffraction patterns and surface SEM images (scale bar represents 50 μm) of YSZ buffer layer. (a) Screen-printed buffer layer on 99.5% alumina substrate fired at 1450 °C for 10 min, (b) sprayed buffer layer on 99.5% alumina substrate fired at 1400 °C for 10 min.

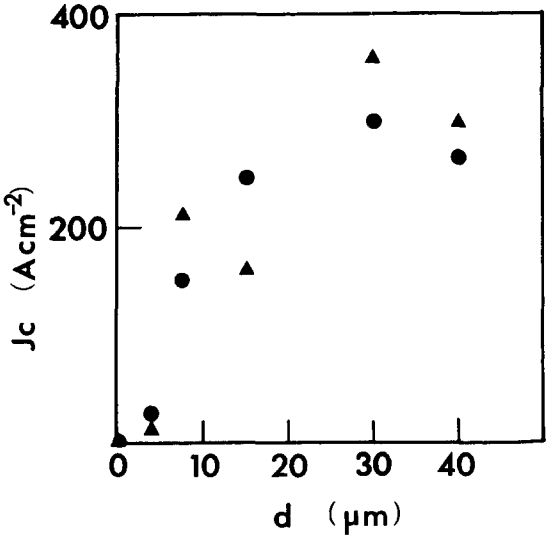

Fig. 5. Variation in critical current density J_c (77 K, 0 T) with thickness of sprayed buffer layer formed on 93% (▲) and 99.5% (●) alumina substrates. The YBCO films were fired at $T_s = 950$ °C for $t = 2$ min ($t_2 = 0$).

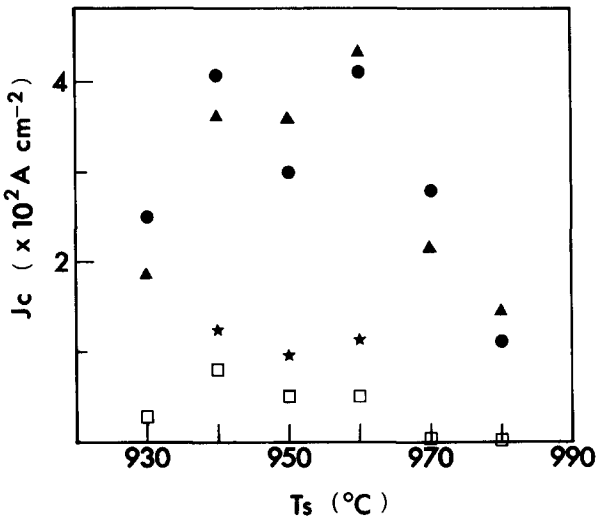

Fig. 6. Critical current density J_c (77 K, 0 T) of YBCO thick films on four kinds of substrate as a function of furnace temperature T_s. □, screen-printed layer on 99.5% alumina; ★, screen-printed layer on alumina green sheet; ●, sprayed layer on 93% alumina; ▲, sprayed layer on 99.5% alumina. Firing time $t = 2$ min ($t_2 = 0$).

Fig. 6 shows the critical current density J_c of 20–25 μm YBCO films as a function of firing temperature T_s, where four kinds of alumina substrate with YSZ buffer layer are used: a screen-printed layer on 99.5% alumina, a screen-printed layer on alumina green sheet, a sprayed layer on 93% alumina, and a sprayed layer on 99.5% alumina. The following features can be seen from this figure. (i) Although the data points are considerably scattered, no significant difference in J_c values between 93% and 99.5% alumina can be seen. (ii) The J_c values of the four series become smaller in the order: sprayed layer on 93% or 99.5% alumina, screen-printed layer on green-sheet, screen-printed layer on 99.5% alumina. This order corresponds to that of the surface roughness and degree of porosity of the layers. As the surface roughness and porosity increase, the J_c value decreases, as discussed later. (iii) The $T_s = 960$ °C films on sprayed buffer layers show a relatively high J_c value of about 400 A cm^{-2}. This value is about two-thirds of that for films on single-crystal YSZ substrates (around 600 A cm^{-2}) [21].

Fig. 7 shows a cross-sectional SEM view and EPMA mapping of Al, Zr, Y, Ba and Cu of the YBCO (20–25 μm) with sprayed buffer layer on 99.5% alumina fired under the conditions of $T_s = 950$ °C and $t = 2$ min ($t_2 = 0$). For this film: (i) the region where certain elements are rich, for example Cu in unbuffered substrate, cannot be observed over the whole region of this film. This implies that the stoichiometric deviation from the (123) phase is suppressed. (ii) Al diffuses from the substrate, across the YSZ layer, into the YBCO film. The concentration gradient of Al in the YBCO film is, however, smaller than that in the buffer layer. (iii) Ba diffuses from YBCO into the

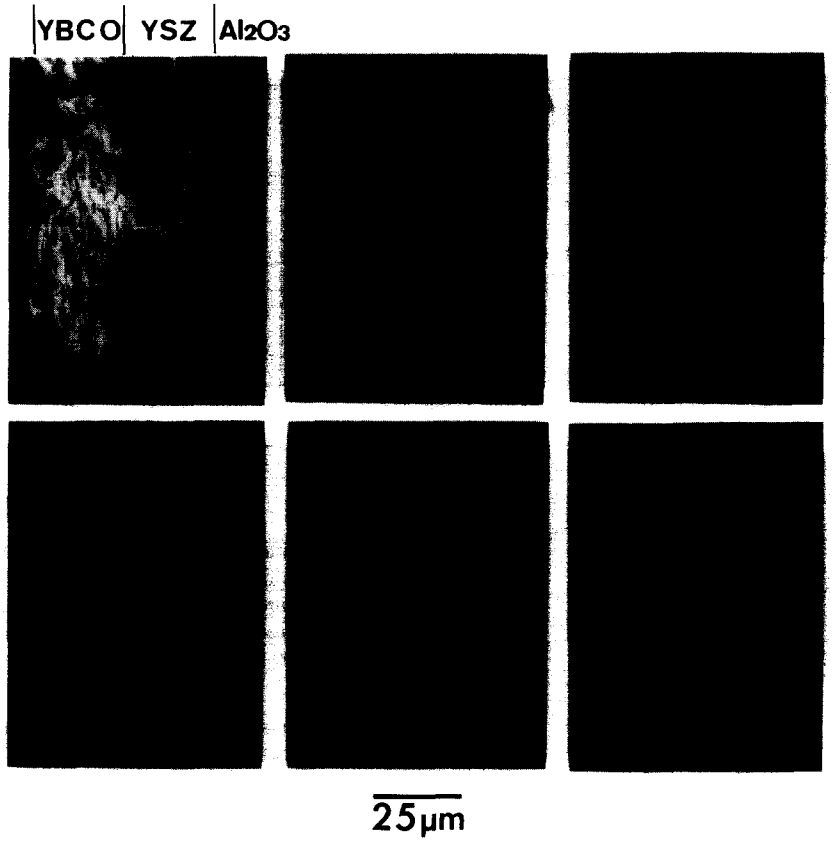

Fig. 7. Cross-sectional SEM view and EPMA mapping of Al, Zr, Y, Ba and Cu for the YBCO thick film with sprayed buffer layer on 99.5% alumina. Element profiles are analyzed on-line. The YBCO film was fired at $T_s = 950\,^{\circ}C$ for $t = 2$ min ($t_2 = 0$).

YSZ buffer layer, which would produce the $BaZrO_3$ layer as suggested by Tabuchi and Utsumi [25]. This layer would suppress the interface reaction by restraining further diffusion of Ba into the buffer layer [26]. These results (i)–(iii) imply that the sprayed YSZ layer (8 mol.% yttria) with its dense structure is very useful for stopping the diffusion of Al. However, the highest J_c value of 400 A cm^{-2} is smaller than that for the film on single-crystal YSZ. This degradation of J_c may be explained as follows: (i) the surface of the sprayed layer is still considerably rougher than that of single-crystal YSZ substrates with surfaces chemically etched to a mirror finish. The rough surface would prevent interconnection between YBCO grains and grain growth of the *ab* plane along the substrate face, i.e. the high degree of *c*-axis orientation, which leads to a high J_c value, is not expected for a rough surface. In fact, the reflection intensity ratios I_{006}/I_{103}, which give a tentative criterion for grain alignment, were 0.5 and 2.0 respectively for two kinds of film on a sprayed YSZ layer and a single-crystal YSZ. (ii) The rough surface also increases the interfacial reaction because of its higher surface area, resulting in a low J_c value. (iii) The sprayed YSZ layer is not 100% dense. The diffusion of Al into the YBCO film would therefore take place due to its porous structure. In fact, a very small amount of Al exists inside the YBCO films, as seen in Fig. 7.

Fig. 8 shows the critical current density J_c at 77 K, 0 T and the room-temperature resistivity ρ as a function of firing time t, $t = 5$, 10, 30, 45 and 60 min ($t_1 = t_2$), for the samples of YBCO film (20–25 μm) with sprayed buffer layer on 99.5% alumina. The firing temperature was kept at the lower temperature of

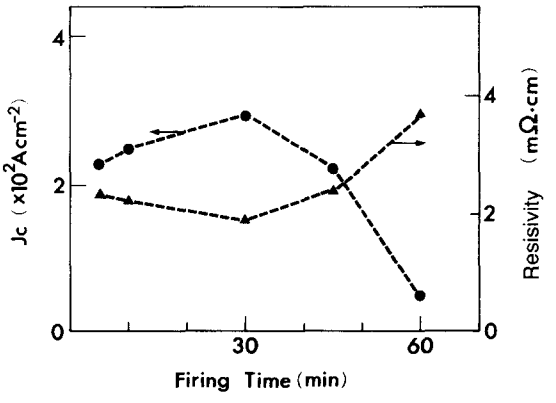

Fig. 8. Variation in critical current density J_c (77 K, 0 T) (●) and room-temperature resistivity ρ (▲) with firing time t ($t = t_1 + t_2$, $t_1 = t_2$) for YBCO thick films on sprayed buffer layer on 99.5% alumina. The YBCO films were fired at $T_s = 920\,^{\circ}C$.

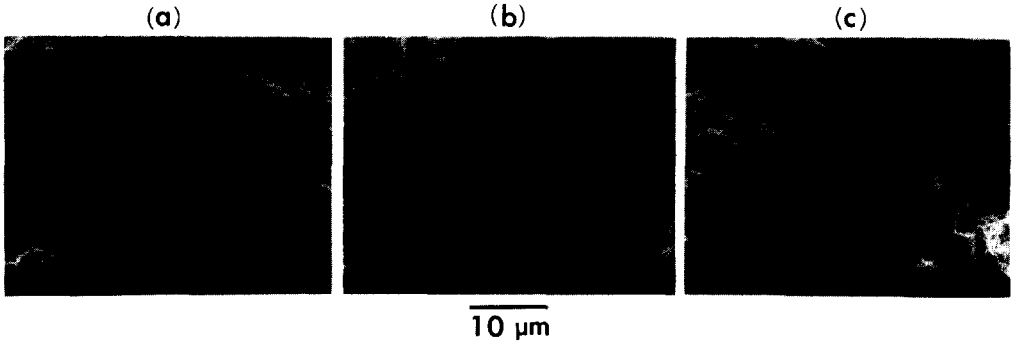

Fig. 9. Surface SEM images of YBCO thick films with sprayed buffer layer on 99.5% alumina fired at T_s = 920 °C. (a) t = 10 min, (b) t = 30 min, (c) t = 60 min.

T_s = 920 °C in order to suppress the interface reaction. Figs. 9(a), 9(b) and 9(c) respectively present surface SEM images of t = 10, 30 and 60 min films. For the t = 10 and 30 min films: (i) the oriented long needle-like crystals with (123) phase are observed over a wide area. (ii) The grain growth is promoted and the plate-like grains with good interconnection are produced with increasing firing time. For the t = 60 min film, oblong-shaped particles with Ba-rich and Cu-poor phase, inferred to be (211) phase, are seen amongst the regions, resulting in a stoichiometric deviation from the (123) phase. The variation of J_c and ρ in Fig. 8 can therefore be explained as follows. As the firing time increases, both the sintering of the film and the connectivity of the YBCO grains improves, lead to the increase in J_c and decrease in ρ. With a further increase of firing time the decomposition of the YBCO phase to the (211) phase, CuO, $BaCuO_2$ and $BaZrO_3$ [27,28] proceeds, leading to the decrease in J_c and increase in ρ.

3.2. Liquid-phase processing method

3.2.1. YBCO films on bare alumina substrates

The 10 μm YBCO films formed on 99.5% alumina were fired at T_s = 1010–1040 °C in steps of 10 °C. These films showed the following: (i) owing to the high heat-treatment, the grain growth was promoted, and the plate-like structure could be seen over a wide area; (ii) all (00l) peaks in the XRD pattern had strong intensity compared with those fired by the solid-phase sintering method; (iii) the resistance–temperature characteristics of some films showed metallic behavior from room-temperaturte to T_c (onset), but no film had zero resistivity above 77 K.

3.2.2. YBCO films on sprayed buffer layers

The 10 μm YBCO films with sprayed YSZ buffer layer (30 μm) on 93% or 99.5% alumina substrate were fired at T_s = 1040, 1050 and 1060 °C. The J_c value and the orientation factor f of these films are given in Table 1. f is given by [29]

$$f = (P - P_0)/(1 - P_0) \quad (2)$$

where P and P_0 are defined by

$$P = \sum I(00l) \Big/ \sum I(hkl), \quad P_0 = \sum I_0(00l) \Big/ \sum I_0(hkl).$$

Here I and I_0 denote the X-ray diffraction intensities for the present and randomly oriented samples respectively. Therefore, f = 1 means a perfect orientation. Fig. 10 presents the XRD pattern of the film fired at T_s = 1050 °C. The inset to this figure gives the surface SEM image. For the films fired by this method, the following features can be seen. (i) The J_c values are considerably higher (900–1300 A cm^{-2}) than those of the films fired by the solid-phase sintering method. (ii) The highest J_c value (approximately 1300 A cm^{-2}) is about two-thirds that of the films on single-crystal YSZ substrates (around 2000 A cm^{-2}) [22]. (iii) All the (00l) peaks have pronounced intensity, indicating that the grain with preferred orientation of the c-axis is promoted. The f value is, however, smaller than that of the YBCO thick film on single-crystal YSZ substrates, where f values are 0.85–0.90 as mentioned in another article [22]. This lesser degree of preferred

Table 1
Critical current density J_c (77 K, 0 T) and orientation factor f of YBCO thick films on two kinds of substrate: Al 93, sprayed buffer layer (30 μm) on 93% alumina; Al 99, sprayed buffer layer (30 μm) on 99.5% alumina. All thick films are about 10 μm thick after firing at T_s = 1040, 1050 and 1060 °C for 2 min.

T_s (°C)	Substrate	J_c (A cm^{-2})	f
1040	Al 93	1100	0.62
	Al 99	1300	0.78
1050	Al 93	1200	0.73
	Al 99	950	0.66
1060	Al 93	900	0.70
	Al 99	1100	0.76

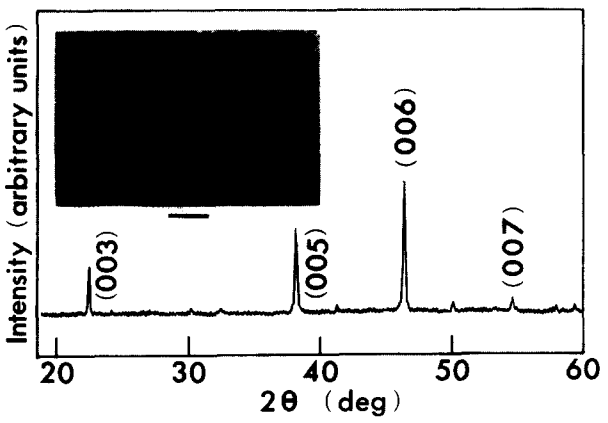

Fig. 10. X-ray diffraction pattern and surface SEM photograph (scale bar represents 20 μm) of YBCO thick film with sprayed buffer layer on 99.5% alumina. The YBCO film was fired at T_s = 1050 °C for 2 min.

orientation, which results in a low J_c value, may be due to the rougher surface of the sprayed layer, as mentioned above. (iv) No significant reflections corresponding to the (211) phase and $BaCuO_2$ are observed in the XRD patterns. (v) A large plate-like grain about 20–30 μm in size and bar-like crystals, identified as the (123) phase by EDXA, are observed. The number of long microcracks, such as those marked A, on the film, however, seem to increase compared with that of the film on YSZ substrate.

It should be emphasized here that the sprayed layer acts as a successful barrier even under conditions of rapid heating, which would induce large thermal stress into the buffer layer, and high temperature heat-treatment of about 1050 °C.

Acknowledgements

The authors would like to express their sincere thanks to I. Hiratsuka and K. Higuma of Meijo University for their technical assistance. This work was supported by a Naito Research Grant.

References

[1] H. Koinuma, T. Hashimoto, T. Nakamura, K. Kishio, K. Kitazawa and K. Fueki, *Jpn J. Appl. Phys., 26* (1987) L761.
[2] K. Tachikawa, N. Sadakata, M. Sugimoto and O. Kohno, *Jpn J. Appl. Phys., 27* (1988) L1501.
[3] P. May, D. Jedamzik, W. Boyle and P. Miller, *Supercond. Sci. Technol., 1* (1988) 1.
[4] N.W. Cody, U. Sudarsan and R. Solanki, *Appl. Phys. Lett., 2* (1988) 1531.
[5] N. Mori, Y. Itoi and M. Okuyama, *Jpn J. Appl. Phys., 28* (1989) L239.
[6] M.L. Kullberg, M.T. Lanagan, W. Wu and R.B. Poeppel, *Supercond. Sci. Technol., 4* (1991) 337.
[7] R.C. Badhani, H. Sing-Mo Tzeng, H.J. Derr and R.F. Bunshan, *Appl. Phys. Lett., 51* (1987) 1277.
[8] I. Shih and C.X. Qiu, *Appl. Phys. Lett., 52* (1988) 748.
[9] A. Gupta, G. Koren, E.A. Geiss, N.R. Moore, E.S.M. O'Sullivan and E.I. Cooper, *Appl. Phys. Lett., 52* (1988) 163.
[10] J.M. Aponte and M. Octavio, *J. Appl. Phys., 66* (1989) 1480.
[11] A. Bailey, S.L. Town, G. Alvarez, G.J. Russel and K.N.R. Taylor, *Physica C, 161* (1989) 347.
[12] M.J. Day, S.D. Sutton, F. Wellhofer and J.S. Abell, *Supercond. Sci. Technol., 6* (1993) 96.
[13] R.P. Gupta, W.S. Khokle, R.C. Dubey, S. Singhal, K.C. Nagpal, G.S.T. Rao and J.D. Jain, *Appl. Phys. Lett., 52* (1988) 1987.
[14] C. Gélinas, P. Lambert, D. Dubé, B. Arsenault and J.R. Cave, *Supercond. Sci. Technol., 6* (1993) 368.
[15] X.M. Li, Y.T. Cho, Y.H. Hu and C.L. Booth, *J. Mater. Sci. Lett., 9* (1990) 669.
[16] H. Koinuma, K. Fukuda, T. Hashimoto and K. Fueki, *Jpn J. Appl. Phys., 27* (1988) L1216.
[17] P. Šťastny, R. Kužel and V. Skácel, *J. Less-Common Met., 164/165* (1990) 464.
[18] T.C. Shields and J.S. Abell, *Supercond. Sci. Technol., 5* (1992) 627.
[19] A. Bailey, K. Sealey, T. Puzzer, G.J. Russel and K.N.R. Taylor, *Mater. Sci. Eng. B 12* (1992) 237.
[20] H. Ohashi, K. Kawabata, M. Niwa and M. Fukuchi, *Jpn J. Appl. Phys., 30* (1991) L32.
[21] Y. Matsuoka, E. Ban and H. Ogawa, *Supercond. Sci. Technol., 2* (1989) 300.
[22] Y. Matsuoka, E. Ban, H. Ogawa and A. Suzumura, *Supercond. Sci. Technol., 4* (1991) 62.
[23] T. Cheung and E. Ruckenstein, *J. Mater. Res., 4* (1989) 1.
[24] L. Madhavrao and R. Rajagopalan, *J. Mater. Sci., 25* (1990) 2349.
[25] J. Tabuchi and K. Utsumi, *Appl. Phys. Lett., 53* (1988) 606.
[26] M.J. Cima, J.S. Schneider and S.C. Peterson, *Appl. Phys. Lett., 53* (1988) 710.
[27] Y. Masuda, K. Matsubara, R. Ogawa and Y. Kawata, *Jpn J. Appl. Phys., 31* (1992) 2709.
[28] Y. Masuda, K. Matsubara, R. Ogawa, Y. Kawata and S. Sakka, *J. Ceram. Soc. Jpn, 101* (1993) 630.
[29] F.K. Lotgerling, *J. Inorg. Nucl. Chem., 9* (1959) 113.